

Selective delipidation of plasma HDL enhances reverse cholesterol transport in vivo

Frank M. Sacks,^{1,*} Lawrence L. Rudel,[†] Adam Conner,[§] Hassibullah Akeefe,[§] Gerhard Kostner,^{**} Talal Baki,[†] George Rothblat,^{††} Margarita de la Llera-Moya,^{††} Bela Asztalos,^{§§} Timothy Perlman,[§] Chunyu Zheng,^{*,§} Petar Alaupovic,^{***} Jo-Ann B. Maltais,[§] and H. Bryan Brewer^{§,†††}

Harvard School of Public Health and Harvard Medical School,^{*} Boston, MA; Wake Forest University Health Sciences,[†] Winston-Salem, NC; Lipid Sciences Incorporated,[§] Pleasanton, CA; Medical University of Graz,^{**} Graz, Austria; Children's Hospital of Philadelphia,^{††} Philadelphia, PA; Tufts University,^{§§} Boston, MA; Oklahoma Medical Research Foundation,^{***} Oklahoma City, OK; Medstar Research Institute,^{†††} Washington Hospital Center, Washington, DC

Abstract Uptake of cholesterol from peripheral cells by nascent small HDL circulating in plasma is necessary to prevent atherosclerosis. This process, termed reverse cholesterol transport, produces larger cholesterol-rich HDL that transfers its cholesterol to the liver facilitating excretion. Most HDL in plasma is cholesterol-rich. We demonstrate that treating plasma with a novel selective delipidation procedure converts large to small HDL [HDL-selectively delipidated (HDL-sdl)]. HDL-sdl contains several cholesterol-depleted species resembling small α , pre β -1, and other pre β forms. Selective delipidation markedly increases efficacy of plasma to stimulate ABCA1-mediated cholesterol transfer from monocyte cells to HDL. Plasma from African Green monkeys underwent selective HDL delipidation. The delipidated plasma was reinfused into five monkeys. Pre β -1-like HDL had a plasma residence time of 8 ± 6 h and was converted entirely to large α -HDL having residence times of 13–14 h. Small α -HDL was converted entirely to large α -HDL. These findings suggest that selective HDL delipidation activates reverse cholesterol transport, in vivo and in vitro. Treatment with delipidated plasma tended to reduce diet-induced aortic atherosclerosis in monkeys measured by intravascular ultrasound. These findings link the conversion of small to large HDL, in vivo, to improvement in atherosclerosis.—Sacks, F. M., L. L. Rudel, A. Conner, H. Akeefe, G. Kostner, T. Baki, G. Rothblat, M. de la Llera-Moya, B. Asztalos, T. Perlman, C. Zheng, P. Alaupovic, J.-A. B. Maltais, and H. B. Brewer. Selective delipidation of plasma HDL enhances reverse cholesterol transport in vivo. *J. Lipid Res.* 2009. 50: 894–907.

Supplementary key words apolipoprotein A-I • kinetics • lipoproteins • nonhuman primates • ABCA1 • SRB1 • pre β -1

The research was conducted at Lipid Sciences (Adam Conner, Hassibullah Akeefe, Timothy Perlman, Dr. Maltais); and at Wake Forest University (Drs. Rudel and Baki), University of Graz (Dr. Kostner), Children's Hospital of Philadelphia (Drs. Rothblat and de la Llera-Moya), Tufts University (Dr. Asztalos), and Oklahoma Medical Research Foundation (Dr. Alaupovic), funded by grants from Lipid Sciences. The monkey atherosclerosis progression study was funded by a National Institutes of Health grant to LLR, HL-24736.

Manuscript received 3 December 2008.

Published, JLR Papers in Press, January 14, 2009.
DOI 10.1194/jlr.M800622-JLR200

In 1951, it was reported that a minor component of the plasma lipoproteins was paradoxically reduced in patients who had coronary heart disease (CHD), in contrast to the bulk of plasma lipoproteins that were notably increased (1). Nine years later, the first prospective studies confirmed that a low plasma HDL cholesterol concentration is a predictor of CHD (2), as have subsequent studies of large populations (3, 4). A low plasma HDL cholesterol concentration is also a predictor of stroke (5). The relation between HDL cholesterol and CHD is strong and consistent among men and women, young and old, and in those with low or high LDL cholesterol concentrations (6); and the influence on HDL cholesterol on risk of CHD persists even during treatment with statins at typical (7) or high doses (8). These findings support the theory that HDL is a component of the lipoprotein system that not only protects against the atherogenic actions of VLDL and LDL, but also may be essential to prevent atherosclerosis even when plasma LDL cholesterol concentration is very low.

HDL transports cholesterol from peripheral tissues, including arterial wall, to the liver directly or by transferring cholesterol to VLDL and LDL in plasma, which eventually deliver much of their cholesterol to the liver (9, 10). The liver can then channel the excess cholesterol for excretion into the bile. This complex process is called reverse cholesterol transport. The step that initiates cholesterol removal from macrophages, the predominant cholesterol-loaded cell type in atherosclerosis, is activation by HDL of cholesterol transporters. Although several cholesterol transporters exist in macrophages and can move cholesterol from inside the cell to HDL, one of them, ABCA1, is required to prevent cholesterol overloading and atherosclerosis. People who lack ABCA1 have abnormal HDL with very low cholesterol content, very low HDL cholesterol concentrations, and suf-

¹To whom correspondence should be addressed.
e-mail: fsacks@hsph.harvard.edu

fer atherosclerosis as early and severely as people with familial hypercholesterolemia (11, 12). People with partial loss of ABCA1 have less severely reduced HDL cholesterol concentration (13). Variation in expression of human ABCA1 in mice predictably affects HDL cholesterol concentrations and atherosclerosis (14, 15).

ABCA1 is activated by pre β -1HDL (16), a flat disk-like complex of phospholipid and a protein, apolipoprotein A-I (17–19). Pre β -1HDL has very little cholesterol (19–21), comprises approximately 5–10% of apoA-I in HDL, and is the main type of HDL that the liver secretes into plasma. After acquiring cholesterol, pre β -1HDL enlarges, takes a spherical shape, and becomes part of the major type of circulating HDL, called α -HDL (17, 20). α -HDL exists in human plasma in several semidiscrete sizes called α -4,3,2, and 1 from small to large (19). Small α -HDL may enlarge by acquiring more cholesterol from cells by other transporters and receptors (22–25). Alpha HDL may be catabolized directly by the liver, kidney, and other steroidogenic tissues; deliver some of its cholesterol to the liver assisted by several enzymes and receptors on the surface of the hepatocyte; or transfer some of its cholesterol to VLDL and LDL, which ultimately are removed from circulation by hepatic LDL receptors (26–28). Effective reverse cholesterol transport requires a continual supply of cholesterol-poor HDL entering the circulation. In animal models of atherosclerosis and in humans with coronary atherosclerosis, giving intravenously complexes of apoA-I and phospholipid, similar to pre β -1 HDL, reduced atherosclerosis (29–33). However, there are obstacles, theoretical and practical, to using pre β -1HDL as a therapy. Conversion of pre β -1 to α -HDL, an essential step in reverse cholesterol transport and the theoretical rationale for HDL treatment, has not been directly observed or quantified in a primate, *in vivo*. ApoA-I is too large to manufacture in sufficient quantities for treatment, and the safety of intravenously infusing nonautologous apoA-I has not been established.

The study asked whether cholesterol-depleted HDL could be generated in human and nonhuman primate plasma by selective delipidation of the predominant, cholesterol-rich α -HDL; whether it is active in cholesterol removal from cholesterol-loaded cells by ABCA1; whether it can be converted to large α -HDL *in vivo*; and whether it could reduce aortic atherosclerosis in a nonhuman primate model of diet-induced atherosclerosis. If the results were positive, selective HDL delipidation would have potential to be a treatment for atherosclerosis.

METHODS

Selective HDL delipidation

Citrated plasma was purchased from local blood banks. Several hundred permutations of delipidation reagents and reagent combinations, and of plasma to delipidation reagent ratios, were screened to identify the parameters for selectively delipidating HDL in plasma. Forward selection criteria included removal of cholesterol from HDL, no change in LDL cholesterol content or size, and stability of lipoproteins in delipidated plasma. Plasma

was mixed with delipidation reagents, sevoflourane (a nonflammable fluorinated ether) and n-butanol. After mixing, plasma and delipidation reagents were bulk separated by gravity and the delipidated plasma was passed through a charcoal column to remove residual delipidation reagents. The plasma was tested using a validated gas chromatographic head space method to ensure that residual delipidation reagents were removed before infusion.

Delipidated plasma was tested using gas chromatography optimized for the detection of residual delipidation reagents. In all delipidation studies of monkey and human plasma, residual levels of the delipidation reagents were below the combined limit of detection, 1.56 ppm, except in one case with human plasma in which the n-butanol was 0.00 ppm and the sevoflurane was 3.40 ppm. Conservative acceptance limits established for a recently concluded human clinical trial were ≤ 20 ppm (mg/L) n-butanol and ≤ 35 ppm (mg/L) fluorinated ether.

Lipid, lipoprotein, apolipoprotein, and enzyme measurements

Lipids and apolipoproteins were measured in plasma before and after delipidation. Cholesterol, nonesterified cholesterol, phospholipid, and triglycerides were measured by enzymatic colorimetry (Wako Chemicals USA, Inc., Richmond, VA). HDL cholesterol was measured by precipitation and enzymatic assay (Wako). LDL cholesterol was measured by direct assay (Wako). VLDL cholesterol was computed by subtracting LDL and HDL cholesterol from the total. ApoB and apoA-I were measured by turbidimetric immunoassay using goat anti-human apoB or apoA-I (Wako). Lipoprotein size and composition were studied by gel permeation chromatography. Plasma or delipidated plasma was applied to Superose 6 column (Amersham Pharmacia), and the indicated fractions were analyzed for cholesterol, phospholipids, and apoA-I.

ApoB lipoproteins may be TG-rich, mostly containing apoC-III or cholesterol-rich that mostly do not contain apoC-III. These types were separated by a combination of immunoprecipitation and immunoaffinity chromatography (34). ApoC-III was measured by electroimmunoassay in plasma, in plasma after precipitation of apoB-containing lipoproteins (VLDL, LDL) by heparin and manganese chloride, and in the precipitate (34).

LCAT and cholesteryl ester transfer protein (CETP) activities were determined as described previously (35, 36). The principle of this method is that the increase in cholesterol ester measured in plasma incubated *in vitro* as a result of LCAT activity is associated with an equivalent molar decrease in free cholesterol. The rate of CETP-mediated transfer of cholesterol ester from HDL to VLDL and LDL is then the difference between the rate of decrease in free cholesterol in whole plasma, and the rate of increase of cholesterol ester in HDL, as a function of time. This assay provides unique information on the interplay between LCAT and CETP reactions by measuring total cholesterol and free cholesterol in total plasma and in apoB-depleted plasma at two time-points.

HDL subtypes produced by selective plasma delipidation, measured by two-dimensional gel electrophoresis

Samples for two-dimensional gel analysis were frozen at -70°C and shipped on dry ice to Tufts University Boston (Boston, MA) for native two-dimensional gel electrophoresis, immunoblotting and image analysis. Each sample received was separated on agarose gel by charge into pre β -, α -, and pre α -mobility particles and on native 3–35% concave gradient polyacrylamide gel by size (5.6 nm to 17.1 nm). Pharmacia High Molecular Weight standard proteins were run in each gel to calculate particle size. Samples were also separated on native 3–16% linear gradient gel in the second dimension to resolve lipid-free apoA-I from pre β HDL. Gels were electro-transferred to nitrocellulose membranes and immuno-

probed for apoA-I with mono-specific polyclonal primary and I¹²⁵ labeled secondary antibodies. Membranes were scanned in a fluoro imager (Molecular Dynamics, Sunnyvale, CA) in X-ray mode. The percent distribution of the signals for each particle was determined by image-analysis using ImageQuant software. ApoA-I contents of the particles were calculated by multiplying the percentiles by the plasma apoA-I level. An in-house reference plasma sample was run with each batch of samples under the same conditions as a control.

Metabolism in mice of LDL from selectively delipidated human plasma

A conventional mouse model of LDL metabolism was used to determine whether selective delipidation affects the clearance of LDL from plasma, a process dependent upon normal recognition of apoB in LDL by LDL receptors, mainly on the liver. If selective delipidation affects the LDL receptor binding region of apoB, or extensively denatures apoB, then clearance from plasma of LDL would be altered. LDL was prepared from 150 ml fresh human citrated plasma obtained from the blood bank at Medical University of Graz, Austria. The lipid concentrations for the plasma were total triglycerides 47 mg/dl, total cholesterol 171 mg/dl, HDL-cholesterol 54 mg/dl, and LDL-cholesterol 108 mg/dl. LDL was prepared by ultracentrifugation within the density range of 1.027–1.063 g/ml. LDL was purified further by density gradient ultracentrifugation, and a narrow band at the appropriate position for LDL protein was harvested. EDTA, 1 mg/ml, was added. LDL, 8 mg protein, was iodinated according to the N-Br succinimide method using 1.5 mCi each of either ¹²⁵I or ¹³¹I. Normal human plasma was spiked with either ¹²⁵I or ¹³¹I LDL. The plasma containing ¹²⁵I LDL was delipidated with the selective delipidation method. Recovery of ¹²⁵I LDL from the delipidated plasma was complete, 102%. Two groups of five mice were each injected with a mixture of the two plasmas. Decay of radioactivity of the LDL in blood after injection was used to quantify the removal and catabolism of LDL from delipidated plasma (¹²⁵I labeled) compared with that of LDL from undelipidated plasma (¹³¹I labeled). Plasma half-lives for LDL from native and delipidated plasma were computed from the disappearance curves for radioactivity (GraphPad Prism) and compared by 2-sample *t*-test. LDL was also prepared from delipidated and undelipidated plasma by ultracentrifugation and applied to a Biogel A-15M column and eluted in phosphate buffered saline at a flow rate of 0.6 cm/h to determine the effect of the delipidation procedure on the size of LDL.

Cholesterol efflux stimulated in cells by selective plasma delipidation

Release of radiolabeled cellular cholesterol to isolated acceptors (e.g., HDL subtypes), or whole serum or plasma was measured at Children's Hospital of Philadelphia as previously described (37). Fu5AH cells were maintained in MEM supplemented with 5% CS and antibiotics. J774 macrophages were maintained in RPMI supplemented with 10% FBS and antibiotics. For efflux experiments 350,000 cells per well were plated in 24-well plates using 0.5 ml of the corresponding growth medium. After 24 h, the growth medium was replaced with 0.5 ml of labeling medium containing 2 μCi [³H]cholesterol/ml and 2 μg/ml of the ACAT inhibitor CP113, 818, and the cells were incubated in this medium for another day. Fu5AH cells were labeled with radioactive cholesterol in MEM containing 0.5% CS and J774 cells were labeled using RPMI containing 1% FBS.

SRB1 mediated cell cholesterol efflux was measured as the fraction of radioactive cholesterol released from Fu5AH cells to 0.2 ml/well of MEM-HEPES containing the test samples as the majority of the cholesterol efflux from these cells is mediated by SRB1. The test samples of HDL or delipidated HDL were loaded

based on a concentration of 15 μg/ml apoA-I. J774 cells were also incubated with 0.2ml/well of MEM-HEPES containing the test samples, Internal control serum was added at 2% v/v in each experiment. ABCA1 mediated efflux was measured as the difference in release of radioactive cellular cholesterol to these media from J774 control macrophages and J774 macrophages up-regulated to express ABCA1 (ABCA1 efflux = FC efflux from up-regulated cells minus FC efflux from control cells). To up-regulate ABCA1 in J774 macrophages, one half of the wells plated with labeled J774 cells were incubated for 16–18 h with 0.5 ml/well of RPMI containing 0.2% BSA, 2 μg/ml CP113, 818 and 0.3 mM cpt-cAMP. Labeled control J774 cells and Fu5AH cells were also incubated for 16–18 h with the same medium without cpt-cAMP. Prior to addition of efflux medium containing the samples to be tested, all cell monolayers were gently washed once with 0.5 ml/well MEM supplemented with 1% BSA and once with 0.5 ml/well MEM. All efflux assays were incubated for 4 h at 37°C and done in triplicate. The fraction of the total radiolabel incorporated into cell lipids released during incubation with the test samples was measured as follows. Radioactive cholesterol incorporated into cell lipids was extracted by incubating a set of triplicate wells of Fu5AH, control J774 and up-regulated J774 cells not exposed to the test serum (T0 cells), overnight with 1 ml isopropanol/well. Total cellular cholesterol label was measured by liquid scintillation counting in aliquots of the isopropanol extracts after drying and resuspension in toluene. Radioactive cholesterol released to test samples after incubation with Fu5AH cells for 4 h or with control and up-regulated J774 cells for 4 h, was measured by scintillation counting of 100 μl aliquots of efflux medium that had been filtered through 0.45 μm-multiscreen filtration plates. All efflux values were corrected by subtracting the small amount of radioactive cholesterol released from triplicate wells of Fu5AH, control and up-regulated J774 cells incubated with serum-free medium.

HDL kinetics in monkeys treated with selectively delipidated monkey plasma

Five monkeys were selected from a larger group of St. Kitts African Green Monkeys (vervets) participating in a dietary fatty acid study at Wake Forest University Medical Center, North Carolina. This primate population, having been on a high-fat diet for 7 years, had developed atherosclerosis, thus providing a model that was genetically similar to man. The plasma used for the delipidation was donor plasma from vervets stored at –20°C since collection. The five recipient monkeys were chosen to be of the same ABO blood group as the plasma donor animals with no irregular isoagglutinins. Research involving these animals was approved by the Wake Forest University Animal Care and Use Committee and conformed to the Wake Forest NonHuman Primate Environmental Enrichment Plan and Policies.

Donor vervet plasma was thawed in the refrigerator overnight. Thawed plasma was pooled, and cryoprecipitate removed by centrifugation (3,500 rpm for 10 min). The vervet plasma was delipidated using the selective delipidation method under aseptic conditions as described above and checked for residual delipidation reagents via gas chromatography prior to infusion.

Delipidated plasma was divided into aliquots by volume to provide the appropriate target dose of apoA-I per monkey based on monkey weight. The monkeys were given one infusion IV of selectively delipidated vervet plasma. The target dosage per recipient monkey was 15–30 mg/kg body weight of apoA-I as measured with vervet specific apoA-I antibodies (38). The target dosage was chosen based on the effective dosages reported in prior atherosclerosis regression studies in animals (29–32), and in humans (33). Animal weights ranged from 6.3 to 8.6 kg, typical for this population of vervets. Plasma was infused at room temperature at a flow rate up to 3 ml/min depending on the tolerance of the animal. The

duration time of infusion ranged from 61 to 84 min. The volume of delipidated plasma given ranged from 95 to 135 ml. The dose of apoA-I delivered per animal was 22 to 23 mg/kg. Diazepam and ketamine were used for anesthesia for the infusion procedure, and ketamine was given periodically for sedation for blood sample collections. Clinical and physiological parameters were measured or monitored. The infusions were well tolerated by the monkeys.

Plasma samples were taken before the infusion, during the infusion, and periodically after the infusion at intervals up to 96 h (Fig. 1). HDL cholesterol, total apoA-I, pre β -1, other pre β , and α -HDL particles were measured as described previously. The concentrations of apoA-I in pre β -1-like, α -3, α -2, and α -1 HDL at the sampling times after infusion were modeled by SAAM II compartmental software by Drs. Zheng and Sacks. An HDL migrating to the pre β -1 position and an HDL migrating to a nearby position not found in native plasma were combined and called "pre β -1-like" HDL. In addition, α -3 and α -4 HDL were combined in this model and called α -3. De novo secretion rates of apoA-I in small (pre β -1-like and α -3), medium (α -2), and large HDL (α -1) in vervets were taken from the previous studies of the investigators (39). The final model consisted of bolus inputs of pre β -1-like, α -3, α -2, and α -1 HDL in the amounts contained in the infusion; conversion of pre β -1-like to α -3, α -2, and α -1; conversion of α -3 to α -2 and to α -1; conversion of α -2 to α -1; and removal of α -2 and α -1 from plasma (Fig. 2). Other pathways were tested including clearance from plasma of pre β -1-like and α -3 HDL, conversion of α -mobility particles to pre β -1 HDL, and conversion of larger to smaller α HDL. Pathways for which rate constants are zero or negligible were eliminated. Data from each monkey were modeled separately. Mean and SD of the rate constants, residence times, and half-lives were computed.

Aortic atherosclerosis in monkeys

Twelve additional monkeys in the atherosclerosis study were entered into a study of 12 weekly treatments of selectively delipidated monkey plasma as described previously for the HDL kinetics study. Intravascular ultrasound (IVUS) of the abdominal aorta was performed before treatment was started and after the final administration of delipidated plasma. The animals were anesthetized, heparin (150–200 units) was given IV prior to catheter introduction, and a small intravascular catheter sheath (2.6–3.0 French or 0.87–1.00 mm) and guidewire were inserted in the right external iliac artery. An IVUS catheter with transducer [Volcano™ Therapeutics In-Vision Intravascular Ultrasound System (K031148) with Volcano Therapeutics Eagle Eye™ 20 MHz Imaging Catheter (K031346)] was advanced proximally and positioned in the aorta above the renal arteries. Nitroglycerin (10–40 mcg per dose) was injected into the aorta to reduce vasoconstriction. The catheter was then retracted by motor at a constant speed of 0.5 mm/sec from this starting point through the right common iliac artery to the sheath. Ultrasonic images were collected with radiofrequency

backscatter triggered by the heart beat of the animal. An image was taken every 0.35 s or 0.18 mm on average. The catheter was removed and the artery sutured. The animals were monitored until fully awake and responsive. The same procedure was followed for pre and posttreatment measurements.

Lesions were located and mapped individually in each frame by manual planimetry to delineate the borders of the lumen and the external elastic lamina. The primary IVUS analysis (planimetry and lesion identification) was conducted by Volcano Therapeutics, Rancho Cordova. Personnel who performed the manual planimetry were blinded to the identity of the monkey and whether the images were from the pre or posttreatment measurement. After planimetry, images were reassembled according to animal and temporal sequence. Lesions on the pre- and posttreatment studies were matched.

Atheroma area was calculated in each frame by subtracting the luminal area from the area bounded by the external elastic membrane (33, 40). Atheroma area includes the intimal and medial layers. Atheroma volume of each lesion was calculated by multiplying the mean atheroma area of the images by its length. Percent atheroma volume, also called atheroma or plaque burden, was computed by dividing the sum of all the atheroma areas by the sum of all of the areas bounded by the external elastic membrane. Changes in atheroma volume and percent atheroma volume are considered to be outcome measures of choice for measuring the effect of a treatment on human coronary arteries using IVUS (40). All lesions that were present in both pre- and posttreatment images were included. We chose this discrete lesion method, analogous to the "most-diseased subsegment" analysis that is often used in the vascular imaging field, because it emphasizes effects on the most diseased areas of the vessel. Because the focal "IVUS-identifiable" lesions were variable in length, all lesions were normalized to lesion length. The lesion was the unit of observation in the statistical analysis.

RESULTS

Selective HDL delipidation of human plasma

In early benchtop development, selective HDL delipidation reduced HDL cholesterol concentration in human plasma from 42 mg/dl to 10 mg/dl, a 77% reduction (N = 51 samples, $P < 0.0001$) (Table 1). LDL cholesterol was not affected. VLDL cholesterol increased from 22 mg/dl to 34 mg/dl ($P < 0.0003$). Plasma total triglycerides decreased by 14%, phospholipids by 15%, and unesterified cholesterol by 10%.

Selective delipidation affected HDL size and composition as shown by gel permeation chromatography (Fig. 3). HDL-

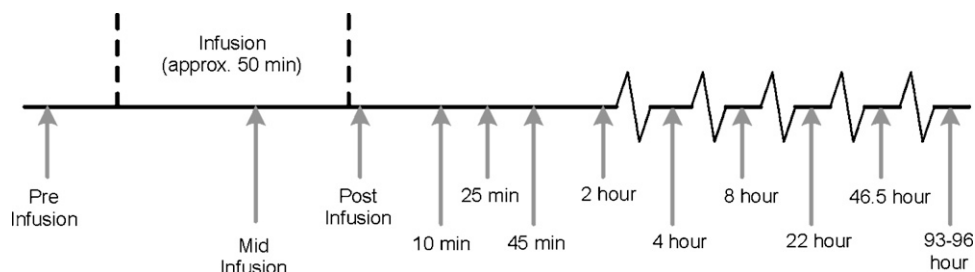


Fig. 1. Design of HDL kinetics study in African Green Monkeys (vervets). Vervet plasma underwent selective HDL delipidation and was infused into five recipient vervets. Arrows depict times of blood sampling.

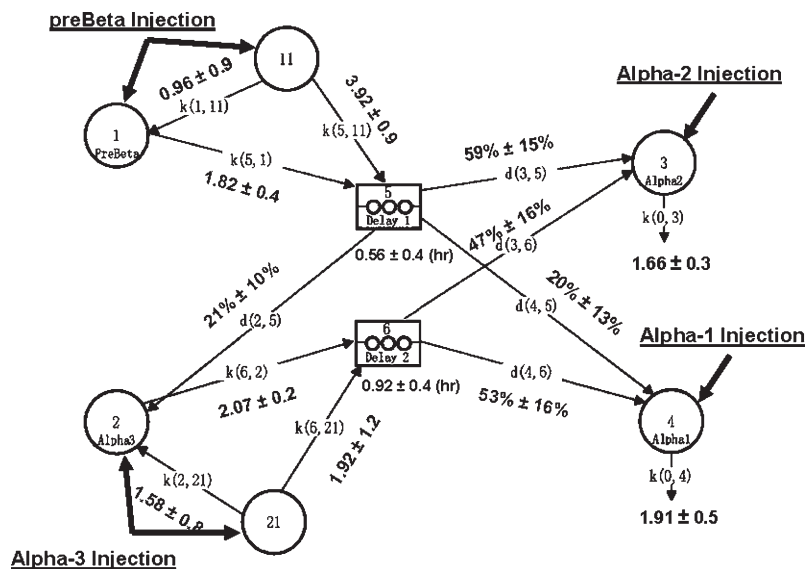


Fig. 2. Compartmental model for metabolism of pre β -1 and α -HDL in African Green Monkeys. Compartment 1: plasma pre β -1 apoA-I. Compartment 11: noncirculating pre β -1 apoA-I. Compartment 2: plasma α -3 apoA-I. Compartment 21: Noncirculating α -3 apoA-I. Compartment 3: plasma α -2 apoA-I. Compartment 4: plasma α -1 apoA-I. Compartments 5 and 6: delay compartments. Selectively delipidated vervet plasma containing pre β -1-like, α -3, α -2, and α -1 HDL was infused into five recipient vervets. Noncirculating compartments 11 and 21 are required for pre β -1 and α -3 HDL because the amount of injected donor apoA-I in these two fractions was significantly higher than the increment in plasma pre β -1 and α -3 HDL observed in recipient monkeys (i.e., only a fraction of injected apoA-I appears in plasma immediately after infusion and the rest appears after a delay). The residence times for the noncirculating compartments of pre β -1 and α -3 HDL are the reciprocals of the rate constants $k(1,11)$ and $k(2,21)$, respectively. Data represented are mean \pm SEM from modeling five monkeys individually. k, rate constants (pools/day); d, delay compartment; % = flux distributions.

sdl was depleted of cholesterol, and the size of HDL-sdl was smaller than in native plasma, as shown by the positions of the HDL phospholipid and apolipoprotein A-I peaks. The HDL-sdl phospholipid and apoA-I peaks were slightly reduced in magnitude compared with native plasma. The position, width, and shape of the VLDL peak were not affected by selective delipidation. The magnitude of the VLDL cholesterol peak was increased. The position of the LDL peak was also unchanged. Apolipoprotein C-III concentration in HDL was decreased by 39% from 6.1 \pm

1.9 to 3.7 \pm 0.2 mg/dl (N = 5 normolipidemic samples, $P < 0.05$).

Removal of cholesterol mass from HDL was strictly proportional to the concentration of HDL cholesterol in plasma before the procedure (Fig. 4, upper panel). Percent removal of cholesterol from HDL was constant over the range of HDL cholesterol concentrations (Fig. 4, lower panel). Thus, the selective delipidation method has similar effectiveness for plasma with high or low HDL cholesterol concentrations, and across a wide range of plasma total cholesterol (50–650 mg/dl) or triglyceride (40–700 mg/dl) concentrations (data not shown).

Selective delipidation markedly decreased α -HDL from 93 \pm 3% to 21 \pm 6%, and produced a mixture of semidiscrete species on the 2-d gels, one approximately in the location of native pre β -1; another near pre β -1 but not present in native plasma, pre β -x; and the smallest type of α , α -4. In native plasma, pre β -1 comprised 6 \pm 3% of total HDL apoA-I immunoreactivity. HDL-sdl was 79 \pm 6% pre β -1-like (N = 6 samples, Fig. 5). The total apoA-I concentration of the samples before delipidation was 112 mg/dl, and 91% was recovered after the procedure. Sham delipidation that included all steps in the delipidation procedure but without the delipidation reagents added produced no changes (data not shown). HDL-sdl has little large- and medium-size α -1 and α -2 HDL that is predominant in native plasma.

LCAT activity is retained in selectively delipidated plasma, whereas CETP activity is markedly reduced by 74% ($P < 0.003$) (N = 6 samples, Table 1).

TABLE 1. Effect of selective HDL delipidation on plasma lipids, apolipoproteins, and LCAT and cholesteryl ester transfer protein (CETP) of human plasma

	Pretreatment (SD)	Posttreatment (SD)	P value
Total cholesterol	159 (24)	141 (22)	<0.0002
Unesterified cholesterol	41 (7)	37 (8)	<0.001
Total triglyceride	164 (121)	141 (108)	0.3
Total phospholipid	186 (26)	158 (27)	<0.0001
HDL-cholesterol	42 (9)	10 (6)	<0.0001
LDL-cholesterol	95 (21)	98 (20)	0.598
VLDL-cholesterol	22 (16)	34 (17)	<0.0003
ApoA-I	109 (14)	81 (15)	<0.0001
ApoB	72 (14)	66 (13)	<0.03
LCAT ^a	7.4 (3.0)	7.9 (3.0)	0.42
CETP ^a	518 (182)	131 (35)	<0.003

N = 51. Units = (mg/dl) except LCAT (μ g/ml/h) and CETP (nmol/ml/h).

^aN = 6.

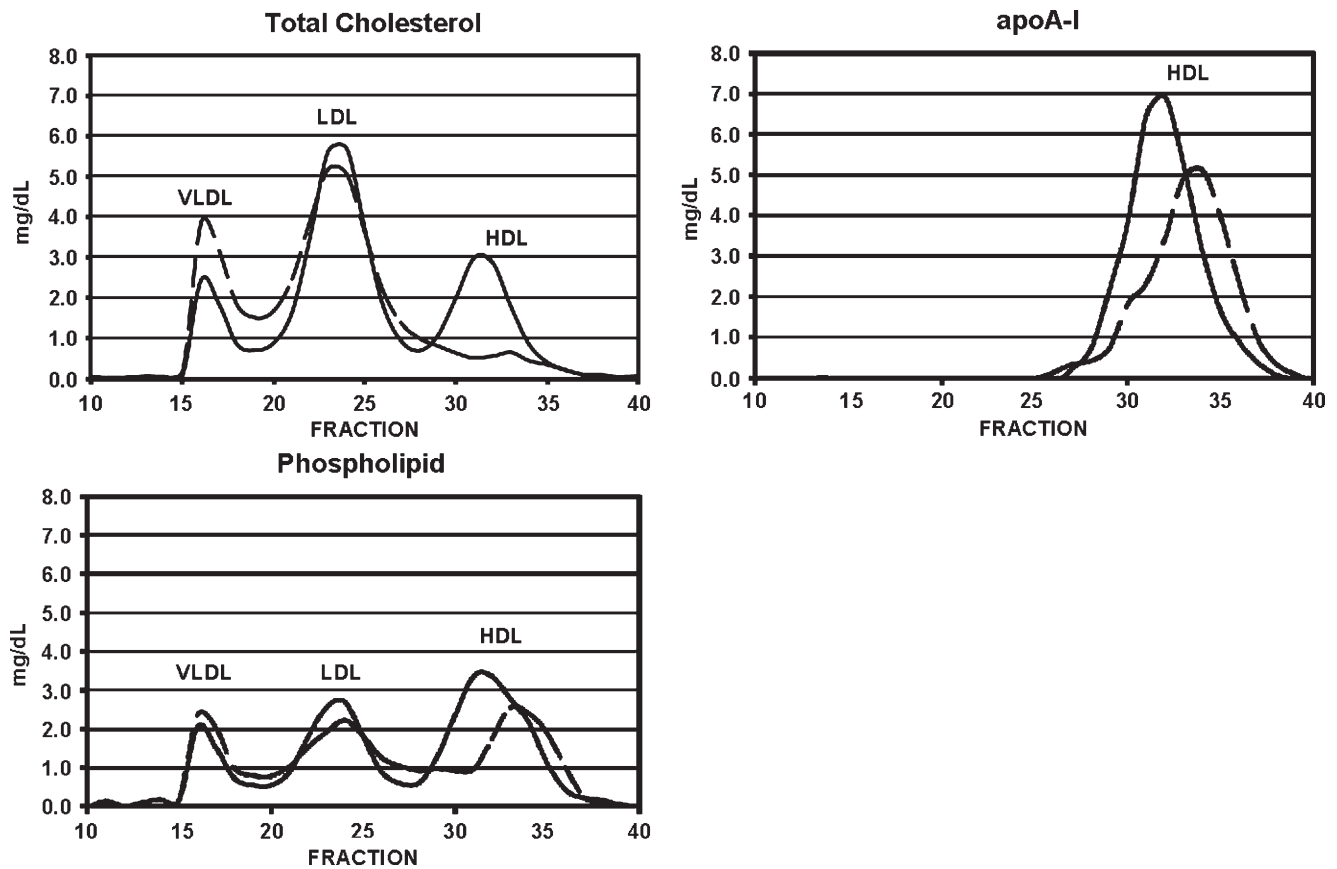


Fig. 3. Effect on lipoprotein size and composition of selective HDL delipidation. Size exclusion chromatography on Superose 6. Solid line: native plasma. Broken line: plasma after selective HDL delipidation. N = 5 normal plasma pools.

ApoB lipoproteins (VLDL, LDL) are composed of TG-rich lipoproteins, usually containing apoC-III and one or more of several other apolipoproteins such as apoC-I, C-II, E, A-II, and D, and called “LpB_c,” and cholesterol-rich lipoproteins that do not have apoC-III and have smaller amounts of the other apolipoproteins, called “LpB” (34). Selective HDL delipidation did not affect the apoB concentrations or proportions of these two types of lipoproteins: LpB_c 20 ± 4 vs. 21 ± 5; LpB 50 ± 10 vs. 44 ± 8 mg/dl (mean ± SD) N = 5 normolipidemic plasma samples. ApoC-III in apoB lipoproteins was also not affected: 4.9 ± 1.2 vs. 4.6 ± 1.3 mg/dl.

Metabolism in mice of LDL from selectively delipidated human plasma

LDL from human plasma that had been selectively delipidated was compared with LDL from native plasma. Selective delipidation had no effect on the size of LDL (**Fig. 6**). The plasma half-life was 4.1 ± 0.4 (SD) h for LDL from delipidated plasma compared with 3.1 ± 0.2 h for LDL from native plasma ($P < 0.01$).

Cholesterol efflux stimulated in cells by selective plasma delipidation

Cholesterol efflux via ABCA1 transporters was improved by the selectively delipidated plasmas for all 16 samples. Compared with sham-processed plasma (no delipidation

reagents), selectively delipidated plasma increased ABCA1 specific cholesterol efflux by 7.1 ± 1.8 (SEM) fold (**Fig. 7**). The median increase was 4-fold, and the range was 1.3 to 27. In contrast, selective delipidation slightly decreased cholesterol efflux via SRB1. Selectively delipidated plasma effluxes cholesterol as well as lipid poor apoA-I, and outperforms HDL-3, a small dense fraction of HDL that contains α - and $\text{pre}\beta$ -1 HDL subtypes.

HDL kinetics in monkeys treated with selectively delipidated monkey plasma

Selective delipidation of pooled donor monkey plasma reduced α -1 from 21% to 1% and α -2 HDL from 35% to 7%, and increased α -3 HDL from 29% to 58% and $\text{pre}\beta$ -like HDL from 15% to 36%. The kinetic behavior of the HDL-sdl particle types is shown for the five monkeys (**Fig. 8**). The infusion of HDL-sdl plasma took approximately 50 min. When the infusion was completed, the average pool size of $\text{pre}\beta$ -1-like particles had increased by 60 mg apoA-I, representing a 2.1-fold increase over baseline. Subsequent reduction in $\text{pre}\beta$ -1-like HDL concentration was biphasic, consisting of a rapid initial phase and a slower later phase. Reciprocal changes occurred in α -1 and α -2 HDL, compared with $\text{pre}\beta$ -1-like HDL. Alpha 1 and 2 HDL concentrations decreased initially during the infusion, reflecting dilution of the monkeys’ plasma compartment by the selectively delipidated donor plasma having low α -1 and α -2

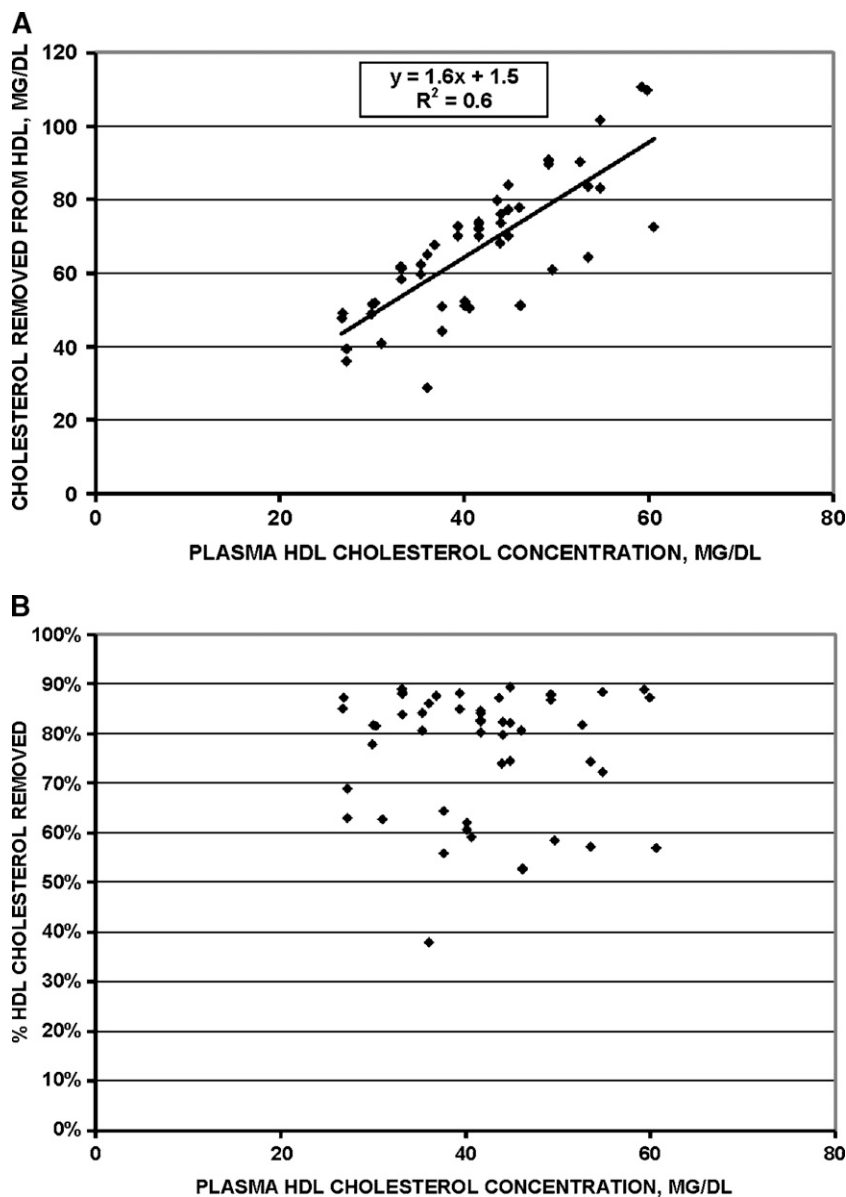


Fig. 4. Efficacy of selective HDL delipidation in 51 human plasma samples. A: mass of cholesterol removed from HDL is proportional to the plasma HDL cholesterol concentration. B: percent of cholesterol removed from HDL is constant across the range of HDL cholesterol concentrations.

HDL concentration as a result of the delipidation process. After infusion, α -1 and α -2 HDL increased rapidly for 2 h, followed by a slow increase to 22 h to a new higher baseline reflecting the amount of infused HDL that is converted to these larger particles.

The kinetic behavior of plasma α -3 concentration, the smallest α -mobility HDL particle in vervets, was intermediate between pre β -1-like HDL and α -1 and α -2 HDL (Fig. 8). Alpha-3 particles initially increased during the infusion, due to the high concentration of α -3 HDL in delipidated plasma. After the infusion ended, α -3 HDL continued to increase to 5 h, and then continuously declined to below baseline at 96 h. Thus, the kinetic pattern after the infusion, a decrease in pre β -1 HDL, an interim increase in α -3 HDL, and a later increase in α -1 and α -2 HDL depicts the reverse cholesterol transport process.

Metabolism of HDL was quantified by kinetic modeling of the apoA-I mass-time curves of pre β -1-like, α -3, α -2, and α -1 HDL (Fig. 2). The concentrations after infusion indicated immediate and delayed appearance of pre β -1-like and α -3 HDL. The delayed appearance required initial noncirculating pools of pre β -1-like and α -mobility particles that later entered the circulation as pre β -1-like or α HDL, respectively. Clearance from plasma of the noncirculating pools was evaluated and found not to fit the data. The data required that all injected pre β -1-like HDL is converted to α HDL, either to the smallest α -mobility HDL, α -3, or directly to the larger α -mobility HDL, α -2 and α -1. Conversion of pre β -1-like to any of these α -types required a delay compartment with a delay time (mean \pm SEM) of 0.56 ± 0.4 h, and conversion of α -3 to α -2 or α -1 HDL involved a delay compartment with mean delay

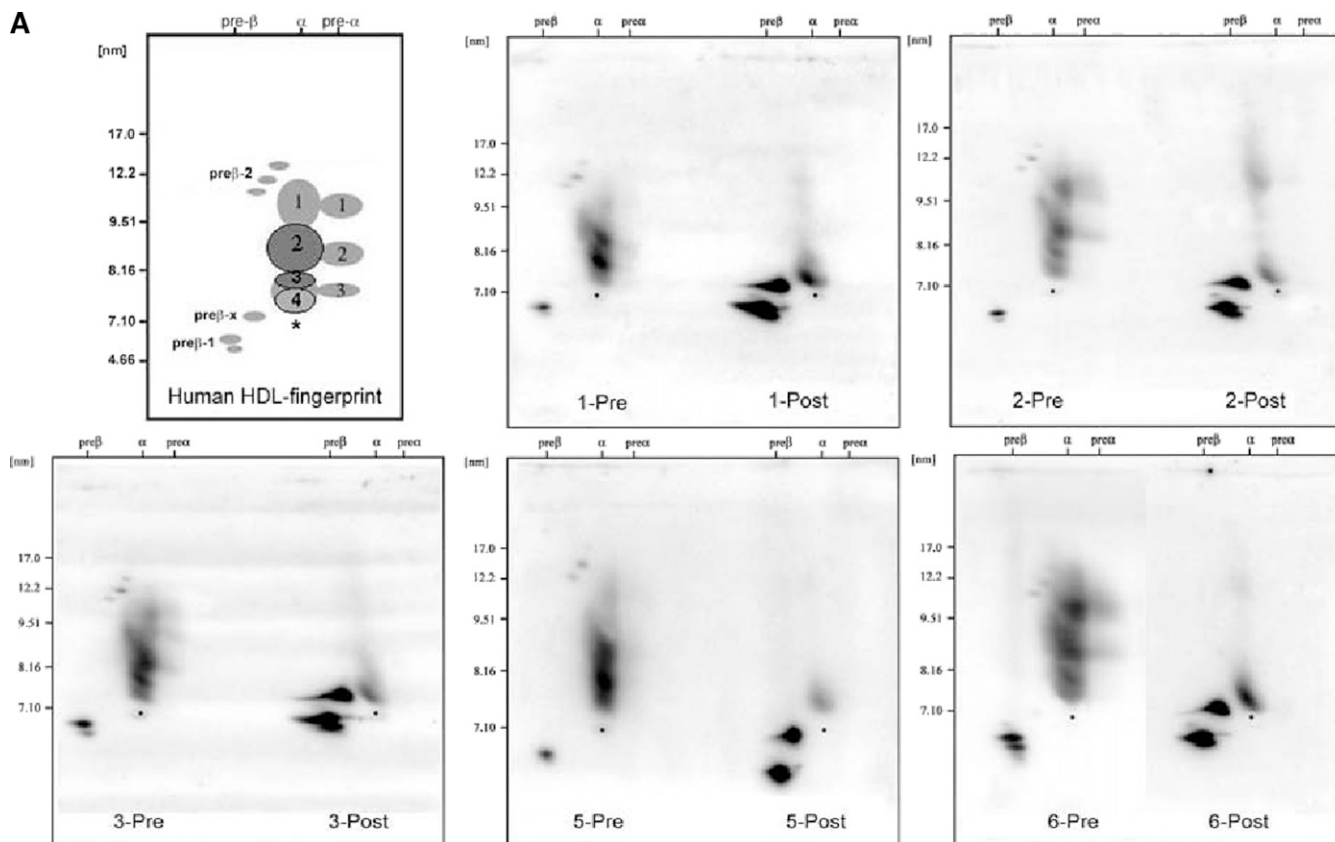


Fig. 5. Selective HDL delipidation of human plasma produces a large shift in HDL types from α to pre β HDL, demonstrated by native two-dimensional gel electrophoresis. **A:** The upper left panel “Human HDL-fingerprint” represents the apoA-I containing (light gray) and apoA-I:A-II containing (dark gray) HDL subpopulations in normolipidemic healthy human subjects in previous studies (16, 19). The asterisk represents the position of human serum albumin, which marks the α -front. The larger α - and pre α -mobility HDL (i.e., α -1, α -2, are lipid-rich spherical particles); the smaller α -3, α -4 HDL are lipid-poor discs or transitional particles. Pre β -2 consists of large, but lipid-poor discoidal particles; pre β -1 consists of small, lipid-poor discs. Pre β -x represents the in-vitro shedding of lipid-poor apoA-I from larger HDL particles caused by the selective delipidation procedure. Lipid content and shape of these bands were determined in previous studies (16, 19). The remaining five panels show HDL in undelipidated plasma (left) and in selectively delipidated plasma from five normal human samples. “Pre” is undelipidated plasma, and “Post” is that of the same plasma selectively delipidated. Samples were subjected to nondenaturing two-dimensional gel electrophoresis and were immunolocalized with human apoA-I antibody. **B:** percentage of HDL apoA-I in pre β and α HDL in six normal subjects, five of whom are shown in the electrophoretograms in the upper panel. Mean \pm SD. Front bars show undelipidated plasma, rear bars show the same plasma sample after selective delipidation. Data determined by scanning the gels shown in the upper panel, and applying the percentages to plasma total apoA-I. The minor pre α 1, 2, and 3, 1–4% of total apoA-I is included with the respective α -HDL in predelipidated samples and was not found postdelipidation. Pre β -2, present only in predelipidated samples, 1% of total apoA-I, is not included. Pre β -x is included with the pre β -1. The mean total apoA-I concentration of the samples before delipidation was 112 mg/dl, and 91% was recovered after the procedure.

time of 0.92 ± 0.4 h. The delay times from pre β -1-like and α -3 compartments were not significantly different. Thus, HDL left the circulation as α -1 or α -2 particles, which did not appear to be converted to one another. Conversion pathways of larger to smaller HDL were tested, representing selective cholesterol uptake by the liver. The model fitting returned rate constants of zero for these pathways. Thus they were not included in the final model shown. Plasma residence times of the particles were similar, 13–14 h. The average coefficients of variation for the fractional catabolic rates of the HDL types after successful model fitting of the data for each monkey were 17% for pre β -1-like ($k[5,1]$), 15% for α -3 ($k[6,2]$), 24% for α -2 ($k[0,3]$), and 38% for α -1 ($k[0,4]$). Sensitivity analysis was performed using in the model only an early period after infusion up to 9 h when concentrations were changing rap-

idly or a later period from 9 h to 95 h when concentrations were changing gradually. The final model and parameter estimates in the time-restricted analyses were similar to those of the full 95 h time period.

Aortic atherosclerosis in monkeys treated with selective HDL delipidation

Twelve monkeys received a pretreatment IVUS study and began weekly treatment with selectively delipidated monkey plasma. Eleven monkeys completed the 12 treatments, and one died after the second treatment for reasons unrelated to the study. Matched pairs of lesions on pre- and posttreatment IVUS studies were identified in 6 of the 11 monkeys. The 6 monkeys had a total of 13 pairs of lesions: 4 lesions in 1 monkey, 2 lesions in 4 monkeys, and 1 lesion in 1 monkey.

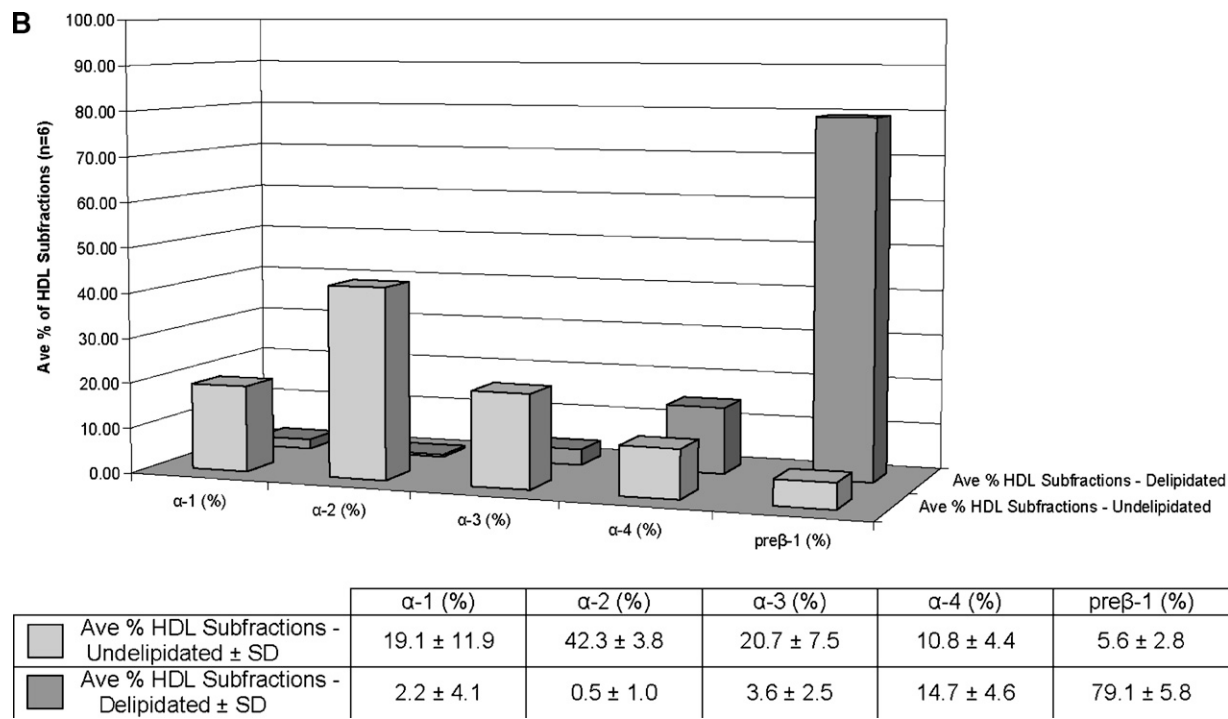


Fig. 5.—Continued.

Atheroma volume decreased significantly by 0.37 mm^3 per mm lesion length, a $6.9 \pm 11.1\%$ reduction ($P = 0.03$) (Table 2). Mean lesion length was unchanged, 11.3 ± 10.0 vs. 11.5 ± 9.9 mm; mean difference 0.2 ± 2.9 , $P = 0.9$. Percent atheroma volume was $31.8 \pm 4.4\%$ pretreatment and $30.3 \pm 5.6\%$ posttreatment, a decrease of 4.4% that is not statistically significant ($P = 0.13$).

DISCUSSION

The main findings of this study are: that treatment of human or monkey plasma with a fluoroether-alcohol solvent selectively delipidates HDL, converting cholesterol-rich α -HDL to a mixture of cholesterol-poor small α , and pre β -like HDLs, termed HDL-sdl; that selectively delipidated plasma has a greatly enhanced ability to stimulate cholesterol efflux from cells by ABCA1 transporters; that HDL-sdl produced by selective delipidation of monkey plasma takes up cholesterol and is converted back to large α -HDL in vivo during 96 h of circulating in the monkeys; and that 12 weekly treatments with selectively delipidated plasma tended to reduce atheroma volume in aortas of monkeys who had diet-induced atherosclerosis. On average, delipidation of 1,100 ml human plasma would be expected to produce 700 to 1,200 mg HDL-sdl, rich in pre β -1-like apoA-I, depending on the initial HDL apoA-I concentration. These findings have implications for understanding HDL metabolism and for a potential treatment of atherosclerosis and other vascular diseases.

LDL concentration, lipid composition, and size were not affected, and its metabolism in mice was normal indicating that the normal interaction of apoB with LDL receptors

that occurs in vivo is preserved. The concentrations of types of apoB lipoproteins, TG-rich (LpB_c) or cholesterol-rich (LpB), were not affected. VLDL retained its size but its cholesterol concentration increased after selective delipidation. It is possible that some of the cholesterol extracted from HDL by the delipidation was taken up by VLDL to attain a thermodynamically more stable distribution, or that CETP transferred cholesterol from HDL to VLDL during the procedure. Some CETP activity was still detected in delipidated plasma once the procedure was complete. Because selective delipidation does not increase VLDL cholesterol in the plasma of mice that do not have CETP, we think this is evidence that there is a mild effect of CETP in human plasma selective delipidation.

Selective delipidation of plasma left HDL with full function to activate ABCA1 in vitro. Selective delipidation removed mainly cholesterol from HDL, preserving most of the phospholipid. Selectively delipidated plasma was at least as effective as lipid-free apoA-I in stimulating ABCA1-mediated cholesterol efflux from cholesterol loaded macrophage-like cells to HDL-sdl. In contrast, selectively delipidated plasma did not enhance SRB1-mediated cholesterol efflux, a mechanism for adding cholesterol to α -HDL. The possible effect of selective delipidation on ABCG1/4-mediated cholesterol efflux, another means of adding cholesterol to α -HDL, was not studied. However, the HDL kinetic findings in monkeys that α -3 HDL in delipidated plasma is converted to α -1 and α -2 HDL, in vivo, is consistent with the action of ABCG1/4 (23–25) or another receptor or transporter with similar function.

Recently, it was shown that ABCA1 and ABCG1/4 can act in a coordinated, sequential, or synergistic way to convert pre β -1 HDL to larger α -HDL particles (25). In essence,

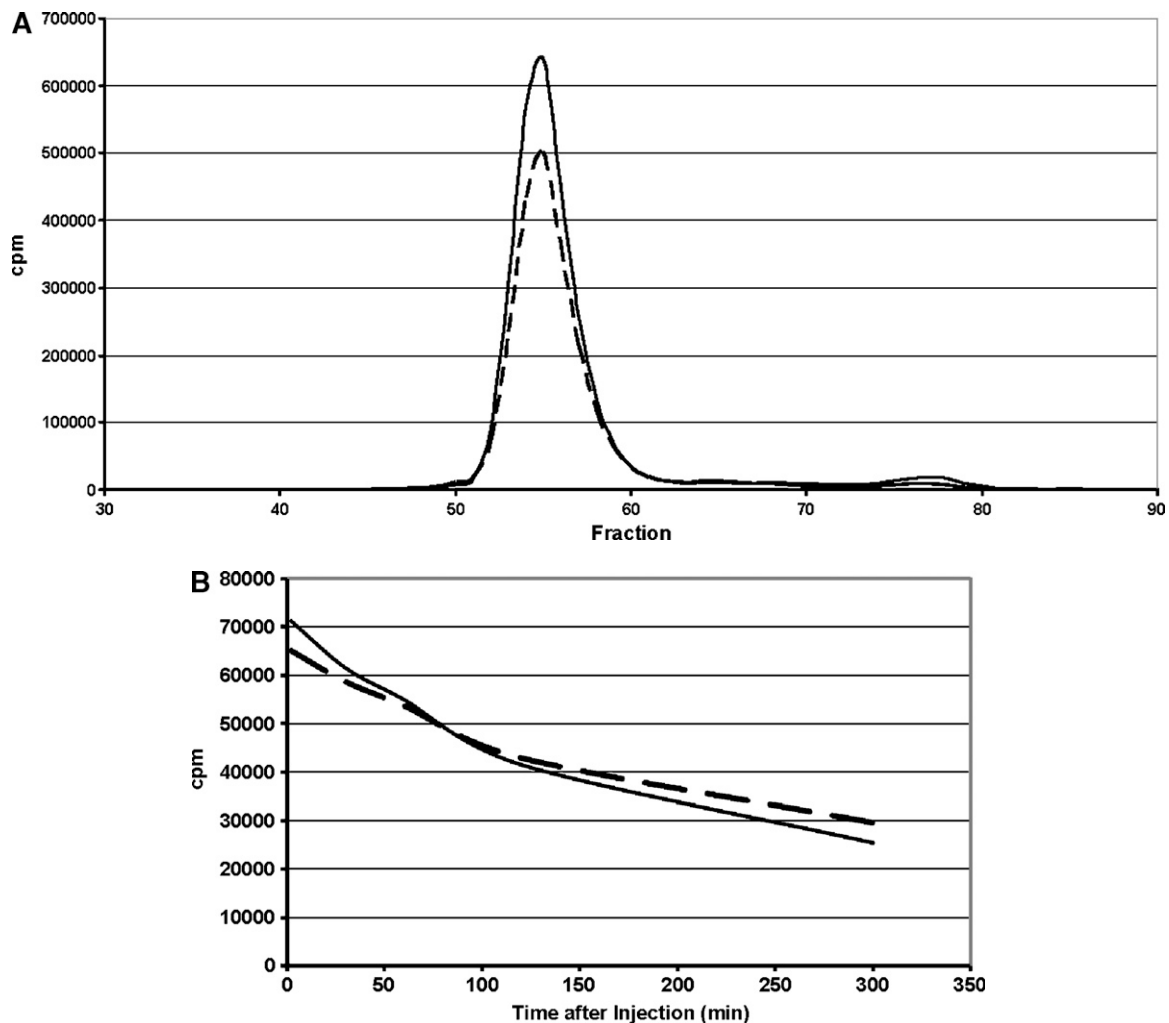


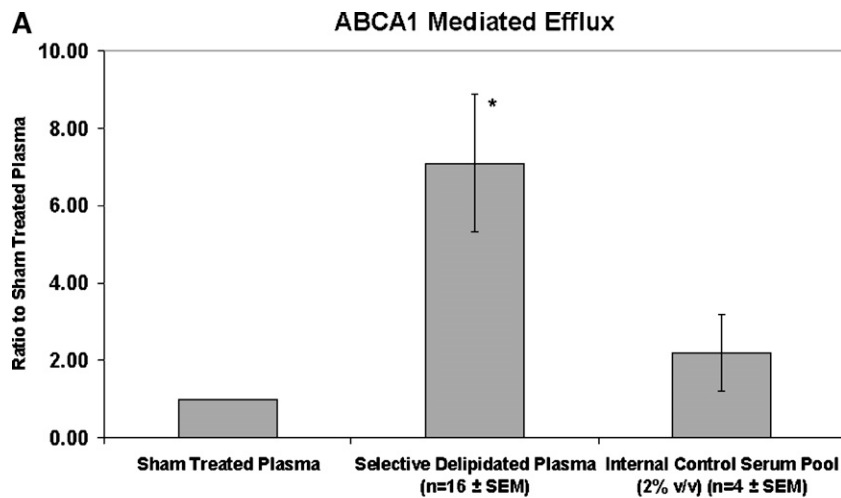
Fig. 6. Metabolism in mice of human LDL from selectively delipidated plasma. A: LDL elution profile by size exclusion chromatography on Biogel A 15m. B: disappearance of radioactivity from LDL after injection into mice. Mean of five mice. Solid lines: ^{131}I -LDL in native human plasma. Broken lines: ^{125}I -LDL in plasma treated with the selective HDL delipidation method. Disappearance curves for radioactivity were fit by GraphPad Prism and half-lives computed. The mean (SD) for $T_{1/2}$ for ^{131}I -LDL was 3.1 ± 0.2 h and for ^{125}I -LDL was 4.1 ± 0.4 h ($P < 0.01$).

ABCA1, when it fulfills its potential to deliver cholesterol to a cholesterol-poor pre β -1 HDL, “hands-off” the small α HDL to ABCG1/4, which then adds cholesterol, converting it to large α -1 and α -2 HDL. The kinetic findings in monkeys could represent *in vivo* evidence for this process due to the fact that pre β -1 HDL do not appear to be converted to the next larger HDL type, α -3, but “jumped” one or two steps, reappearing in plasma as a α -1 and α -2 HDL. These pathways were needed for satisfactory fitting of the compartmental model to the data. In fact, the metabolic products of pre β -1 HDL that appear in plasma include all three α -HDLs; the percentage distribution from pre β -1 HDL to specific α -HDL types could reflect the availability of ABCG1/4 or SRB1 relative to ABCA1 and could be influenced by the excess amount of cellular cholesterol that could drive the efflux system (41).

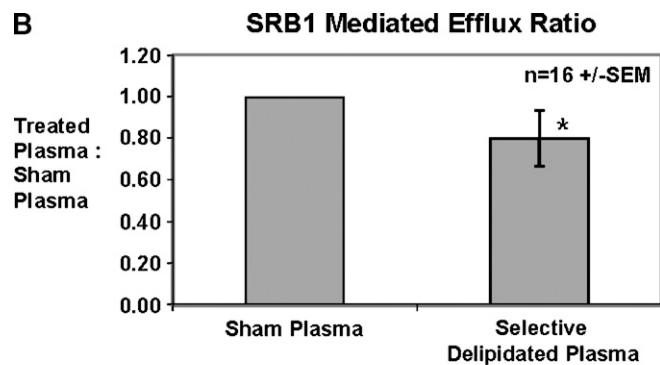
The kinetic findings suggest that none of the HDL infused with selectively delipidated plasma is wasted (i.e., directly cleared) and not available for reverse cholesterol transport. All pre β -1-like HDL are converted to α -HDL,

and all α -3 HDL are converted to α -1 and α -2 HDL, and these conversions occur through a sequestration compartment, the “delay” pool. It is possible that the pre β -1-like and α -3 HDL, infused in large amounts relative to that in native plasma, may have overloaded cellular cholesterol transporters or receptors and caused pre β -1 and α -3 particles to enter a sequestered space right after the infusion. However, a substantial sequestration compartment was found in a tracer study using small amounts of radioiodinated HDL (39). The sequestration compartment may represent a normal docking mechanism for keeping small HDL on the vascular endothelium, in the subintimal space or even inside cholesterol-loaded cells (42) until cholesterol transfer can occur, launching the α -1 and α -2 particles into the circulation. This has an important physiological and potential therapeutic meaning because nascent or infused pre β -1 and small α -HDL particles are efficiently and completely used for reverse cholesterol transport.

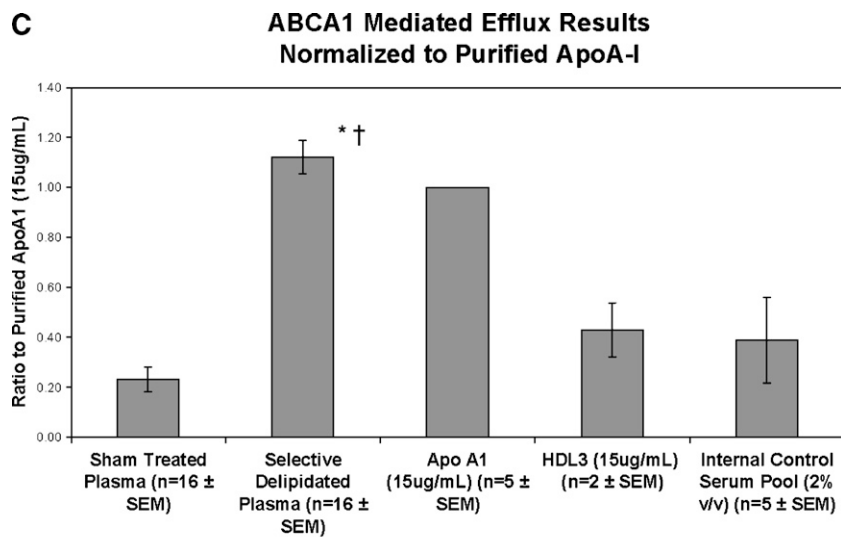
It is not possible to know how closely the kinetic findings portray normal HDL metabolism or whether they are spe-



* $p < 0.001$ versus Sham Plasma or Internal Control Serum



* $p < 0.05$ versus sham plasma



* $p < 0.001$ versus sham plasma; † $p < 0.003$ versus HDL3

Fig. 7. Cell cholesterol efflux caused by selectively delipidated plasma. A: ABCA1 mediated efflux. Ratio of selectively delipidated or native plasma to sham delipidated plasma. Compared with sham processed plasma (no delipidation reagents), selectively delipidated plasma increased ABCA1 specific cholesterol efflux by 7.1 ± 1.8 (SEM) fold. The median increase was four-fold, and the range was 1.3 to 27. Control serum is an internal standard and is added at 2% v/v, and results are typical. B: SRB1 mediated efflux. Ratio of selectively delipidated to sham delipidated plasma. C: ABCA1 mediated efflux. Effects of selectively delipidated plasma, native plasma (sham delipidated control), apoA-I, and HDL-3. Vertical axis units are efflux ratio of samples to purified human apoA-I. N = 16 plasma samples, mean \pm SEM.

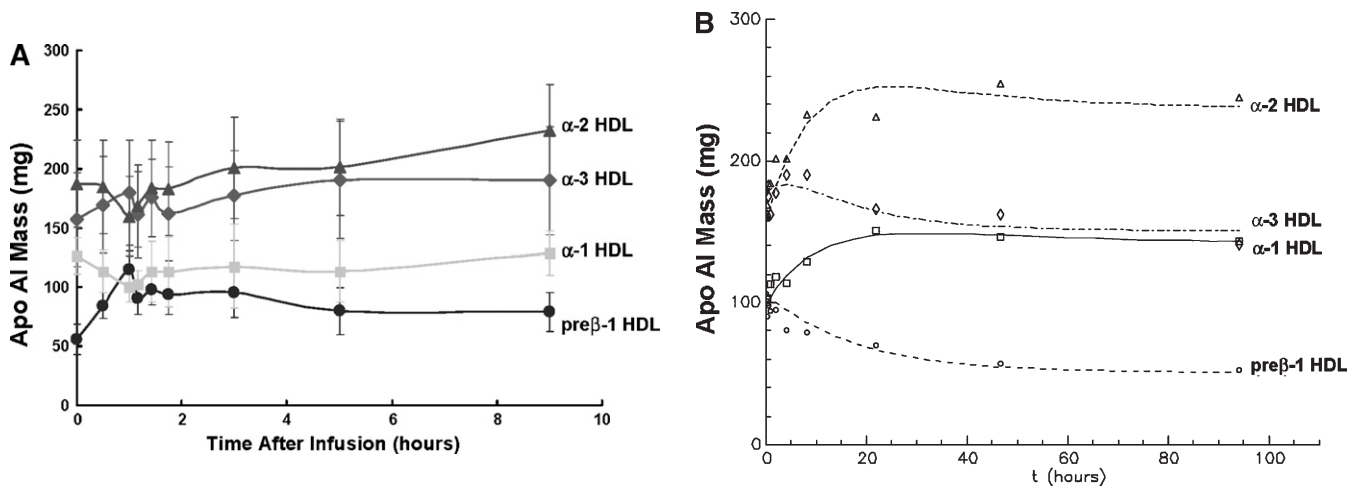


Fig. 8. A: Pre β -1 and α HDL apoA-I plasma mass (pool size) in vervets at baseline and immediately after infusion of selectively delipidated vervet plasma (mean \pm SEM of five vervets) B: Modeling fitting of pre β -1 and α -HDL apoA-I mass after infusion. Symbols are the masses of apoAI in each HDL type. Lines are fitted curves to the data determined by kinetic modeling using the model in Fig. 2. Mean of five vervets. "Pre β -1" includes pre β -x as shown in Fig. 5.

cific to the experimental conditions designed for therapy (i.e., the HDL particles, termed HDL-sdl, produced by the selective delipidation procedure). In vervets, kinetics of radioiodinated α -HDL tracers with small, medium, or large sizes share several key features with the present tracee kinetic study (39). Both studies found that conversion of HDL particle types is unidirectional from small to large, and that small HDL is quantitatively converted to large HDL, none of it cleared directly. The radioiodinated HDL study found that the conversion pathway from small to medium or large HDL has a required noncirculating compartment in which some small HDL is converted directly to large HDL and some is converted to medium HDL (39). This process resembles the delay compartment used in the present study in which α -3 HDL is converted to either α -2 or α -1 HDL. Human studies of HDL metabolism that used radioiodinated HDL also described two-pool models having noncirculating and circulating components (43). The radioiodinated study determined that medium-size HDL is not converted to large-size HDL, analogous to α -2 not being converted to α -1 HDL in the present study. Finally, neither the radioiodinated study nor the present study could identify conversion of larger to smaller HDL such as mediated by SR-B1. Thus, the concordance of findings between these two different studies of HDL metabolism in vervet monkeys suggests that the present study may have identified some of the normal pathways of HDL as it circulates in plasma.


In contrast to the concordant findings between tracer and tracee studies with respect to the metabolic pathways for plasma HDL metabolism, the present study estimated lower residence times for α -HDL, 13–14 h, less than half that found in the radioiodinated HDL study (39). A tracee kinetic study of apoA-I infusion in humans showed that the clearance rate from plasma of apoA-I increased with the amounts of apoA-I given (44). The authors interpreted this finding as direct first-pass clearance of infused apoA-I. However, the present study found no evidence for rapid clearance of infused apoA-I. It is possible that the large amount of pre β -1 and α -3 HDL infused in delipidated plasma stimulated the rate of its own metabolism through normal not aberrant pathways. A kinetic study of pre β -1 and α -HDL in normal people, using primed-constant infusion of trideuterated leucine, reported conversion times for pre β -1 to α -HDL of 15 min, rapid back-conversion of α - to pre β -1 HDL, and a plasma residence time for pre β -1 of approximately 4 days (45). However, the tracer enrichments for pre β -1 and α -HDL appeared in plasma at the same time and had parallel time curves. Because the tracer technique did not provide disappearance curves for pre β -1 and α -HDL, the parallel time curves for tracer appearance of apoA-I in pre β -1 and α -HDL could just as well be interpreted as independent pools with different residence times. There is an unfortunate paucity of data on kinetics of pre β -1 HDL in humans.

TABLE 2. Effect of selective HDL delipidation on aortic atheroma in monkeys

	Total atheroma volume			Percent atheroma volume		
	Pretreatment	Posttreatment	% change	Pretreatment	Posttreatment	% Change
Mean	5.63	5.25	-6.9%	31.78	30.26	-4.4%
SD	1.27	1.41	11.1%	4.41	5.61	14.8%
	<i>P</i> = 0.03			<i>P</i> = 0.13		

N = 13 lesions, matched on pre- and posttreatment Intravascular ultrasound (IVUS) studies, in six monkeys. Total atheroma volume = mm³/mm lesion length. Percent atheroma volume = %.

Infusion of selectively delipidated monkey plasma tended to improve aortic atherosclerosis in monkeys that had developed atherosclerosis on a high saturated fat diet for 7 years. This finding is consistent with a human trial of apoA-I Milano in coronary atherosclerosis (33), and several animal models of atherosclerosis in which complexes of apoA-I and phospholipid similar to pre β -1 HDL were given intravenously (29–32). A strength of this study includes its use of an amount of apoA-I and several infusions that are suitable for scaling-up for human studies. The strictly blinded protocol for identifying aortic lesions provided an unbiased identification and analysis of lesions. Infusion of pre β -1 HDL would be expected to directly reduce atheroma volume, the endpoint that significantly improved. Percent atheroma volume tended to decrease although not significantly. Percent atheroma volume is related to remodeling of plaque as much as to reduction in volume, and may be viewed as a second-order effect of the reduction in atheroma volume itself. Limitations include the absence of a control group of monkeys receiving a sham infusion and the small number of monkeys that had discrete aortic lesions visualized on pre- and posttreatment IVUS studies. This is the first study to our knowledge to use IVUS to study aortic atherosclerosis in monkeys. Because all of the monkeys had aortic atherosclerosis on histological analysis, it is likely that the technique of IVUS utilized in this study was not optimal for this purpose.

In conclusion, selective delipidation of HDL in human or monkey plasma generates cholesterol-depleted HDL, resembling pre β -1 and small α species that are active in removing cholesterol from cells. Infusion into monkeys of selectively delipidated monkey plasma containing these small HDL rapidly converts them to larger α -2 and α -1 HDL during the first day, and more slowly for at least another day, suggesting the possibility that selective delipidation induces a more active process of reverse cholesterol transport lasting 2 days or more. The IVUS results, suggesting that the treatment improved aortic atherosclerosis in the monkeys, support the clinical significance of the HDL kinetic results. Thus, selective HDL delipidation has potential as a therapy for atherosclerosis, and a Phase 1 pilot trial has been completed in patients with CHD. Potential therapeutic applications for selective HDL delipidation also include acute coronary syndrome, acute stroke (46), coronary ischemia-reperfusion injury (47, 48), and in-stent stenosis (49). 

We would like to gratefully acknowledge the following people at Lipid Sciences without whom this work wouldn't have been possible: Barrett C. Craner, Costa Gillespie, Robert Michaloski, and Moiz Kitabwalla. The talented technical research team that made the monkey studies possible included Kathryn Kelley, Janet Sawyer, and Ramesh Shah with capable veterinarian support from Drs. Jeanne Wallace and Kylie Kavanagh.

Drs. Sacks, Kostner, Alaupovic, and Brewer were members of the Scientific Advisory Board, Lipid Sciences, and had stock options or stock. Drs. Sacks, Rudel, Kostner, Rothblat, Asztalos, Zheng, and Alaupovic were consultants to Lipid Sciences. Adam Conner, Hassibulah Akeefe, Timothy Perlman,

and Dr. Maltais were employees of Lipid Sciences. Dr. Brewer was Chief Scientific Director and member of the Board of Directors, Lipid Sciences.

REFERENCES

- Barr, D. P., E. M. Russ, and H. A. Eder. 1951. Protein-lipid relationships in human plasma. II. In atherosclerosis and related conditions. *Am. J. Med.* **11**: 480–493.
- Gofman, J. W., W. Young, and R. Tandy. 1966. Ischemic heart disease, Atherosclerosis, and longevity. *Circulation.* **34**: 679–697.
- Miller, G. J., and N. E. Miller. 1975. Plasma-high-density-lipoprotein concentration and development of ischaemic heart-disease. *Lancet.* **1**: 16–19.
- Gordon, D. J., J. L. Probstfield, R. J. Garrison, J. D. Neaton, W. P. Castelli, J. D. Knoke, D. R. Jacobs, S. Bangdiwala, and H. A. Tyroler. 1989. High-density lipoprotein cholesterol and cardiovascular disease: four prospective American studies. *Circulation.* **79**: 8–15.
- Sanossian, N., J. L. Saver, M. Navab, and B. Ovbiagele. 2007. High density lipoprotein cholesterol. An emerging target for stroke treatment. *Stroke.* **38**: 1104–1109.
- Sacks, F. M., A. M. Tonkin, T. Craven, M. A. Pfeffer, J. Shepherd, A. Keech, C. D. Furberg, and E. Braunwald. 2002. Coronary heart disease in patients with low LDL cholesterol: benefit of pravastatin in diabetics and enhanced role of HDL-cholesterol and triglycerides as risk factors. *Circulation.* **105**: 1424–1428.
- Cholesterol Treatment Trialists' Collaborators. 2005. Efficacy and safety of cholesterol-lowering treatment: prospective meta-analysis of data from 90 056 participants in 14 randomised trials of statins. *Lancet.* **366**: 1267–1278.
- Barter, P., A. M. Gotto, J. C. Larosa, J. Maroni, M. Szarek, S. M. Grundy, J. J. Kastelein, V. Bittner, and J. C. Fruchart. 2007. HDL cholesterol, very low levels of LDL cholesterol, and cardiovascular events. *N. Engl. J. Med.* **357**: 1301–1310.
- Brewer, H. B., Jr. 2004. Increasing HDL cholesterol levels. *N. Engl. J. Med.* **350**: 1491–1494.
- Rader, D. J. 2006. Molecular regulation of HDL metabolism and function: implications for novel therapies. *J. Clin. Invest.* **116**: 3090–30100.
- Assmann, G., A. Von Eckardstein, and H. B. Brewer. 1995. Familial high density lipoprotein deficiency: Tangier disease. In *The Metabolic and Molecular Bases of Inherited Disease*. C. R. Scriver, A. L. Beaudet, W. S. Sly, D. Valle, editors. McGraw-Hill, New York, NY. 2053–2072.
- Serfaty-Lacrosniere, C., F. Civeira, A. Lanzberg, P. Isaia, J. Berg, E. D. Janus, M. P. Smith, P. H. Pritchard, J. Frohlich, R. S. Lees, et al. 1994. Homozygous Tangier disease and cardiovascular disease. *Atherosclerosis.* **107**: 85–98.
- Brunham, L. R., R. R. Singaraja, and M. R. Hayden. 2006. Variations on a gene: rare and common variants in ABCA1 and their impact on HDL cholesterol levels and atherosclerosis. *Annu. Rev. Nutr.* **26**: 105–129.
- Singaraja, R. R., C. Fievet, G. Castro, E. R. James, N. Hennuyer, S. M. Clee, N. Bissada, J. C. Choy, J. C. Fruchart, B. M. McManus, et al. 2002. Increased ABCA1 activity protects against atherosclerosis. *J. Clin. Invest.* **110**: 35–42.
- Joyce, C. W., M. J. Amar, G. Lambert, B. L. Vaisman, B. Paigen, J. Najib-Fruchart, R. F. Hoyt, Jr., E. D. Neufeld, A. T. Remaley, D. S. Fredrickson, et al. 2002. The ATP binding cassette transporter A1 (ABCA1) modulates the development of aortic atherosclerosis in C57BL/6 and apoE-knockout mice. *Proc. Natl. Acad. Sci. USA.* **99**: 407–412.
- Asztalos, B. F., E. J. Schaefer, K. V. Horvath, S. Yamashita, M. Miller, G. Franceschini, and L. Calabresi. 2007. Role of LCAT in HDL remodeling: investigation of LCAT deficiency states. *J. Lipid Res.* **48**: 592–599.
- Yokoyama, S. 2006. Assembly of high density lipoproteins. *Arterioscler. Thromb. Vasc. Biol.* **26**: 20–27.
- Curtiss, L. K., D. T. Valenta, N. J. Hime, and K. A. Rye. 2006. What is so special about apolipoprotein A-I in reverse cholesterol transport? *Arterioscler. Thromb. Vasc. Biol.* **26**: 12–19.
- Asztalos, B. F., M. de la Llera-Moya, G. E. Dallal, K. V. Horvath, E. J. Schaefer, and G. H. Rothblat. 2005. Differential effects of HDL subpopulations on cellular ABCA1 and SRB-1 mediated cholesterol efflux. *J. Lipid Res.* **46**: 2246–2253.

20. Kunitake, S. T., K. J. La Sala, and J. P. Kane. 1985. Apolipoprotein A-I-containing lipoproteins with pre-beta electrophoretic mobility. *J. Lipid Res.* **26**: 549–555.
21. Rye, K. A., and P. J. Barter. 2004. Formation and metabolism of prebeta-migrating, lipid-poor apolipoprotein A-I. *Arterioscler. Thromb. Vasc. Biol.* **24**: 421–428.
22. Rothblat, G. H., M. de la Llera-Moya, V. Atger, G. Kellner-Weibel, D. L. Williams, and M. C. Phillips. 1999. Cell cholesterol efflux: integration of old and new observations provides new insights. *J. Lipid Res.* **40**: 781–796.
23. Wang, N., D. Lan, W. Chen, F. Matsuura, and A. R. Tall. 2004. ATP-binding cassette transporters G1 and G4 mediate cellular cholesterol efflux to high-density lipoproteins. *Proc. Natl. Acad. Sci. USA.* **101**: 9774–9779.
24. Kennedy, M. A., G. C. Barrera, K. Nakamura, A. Baldan, P. Tarr, M. C. Fishbein, J. Frank, O. L. Francone, and P. A. Edwards. 2005. ABCG1 has a critical role in mediating cholesterol efflux to HDL and preventing cellular lipid accumulation. *Cell Metab.* **1**: 121–131.
25. Gelissen, I. C., M. Harris, K. A. Rye, C. Quinn, A. J. Brown, M. Kocx, S. Cartland, M. Packianathan, L. Kritharides, and W. Jessup. 2006. ABCA1 and ABCG1 synergize to mediate cholesterol export to apoA-I. *Arterioscler. Thromb. Vasc. Biol.* **26**: 534–540.
26. Ouguerram, K., M. Krempf, C. Maugeais, P. Maugeere, D. Darmaun, and T. Magot. 2002. A new labeling approach using stable isotopes to study in vivo plasma cholesterol metabolism in humans. *Metabolism.* **51**: 5–11.
27. Schwartz, C. C., J. M. VandenBroek, and P. S. Cooper. 2004. Lipoprotein cholesteryl ester production, transfer, and output in vivo in humans. *J. Lipid Res.* **45**: 1594–1607.
28. Eriksson, M., L. A. Carlson, T. A. Miettinen, and B. Angelin. 1999. Stimulation of fecal steroid excretion after infusion of recombinant proapolipoprotein A-I. Potential reverse cholesterol transport in humans. *Circulation.* **100**: 594–598.
29. Chiesa, G., E. Monteggia, M. Marchesi, P. Lorenzon, M. Laucello, and V. Lorusso. 2002. Recombinant apolipoprotein A-I_{Milano} infusion into rabbit carotid artery rapidly removes lipid from fatty streaks. *Circ. Res.* **90**: 974–980.
30. Badimon, J. J., L. Badimon, and V. Fuster. 1990. Regression of atherosclerotic lesions by high density lipoprotein plasma fraction in the cholesterol-fed rabbit. *J. Clin. Invest.* **85**: 1234–1241.
31. Shah, P. K., J. Yano, O. Reyes, K. Y. Chyu, S. Kaul, C. L. Bisgaier, S. Drake, and B. Cercek. 2001. High-dose recombinant apolipoprotein A-I Milano mobilizes tissue cholesterol and rapidly reduces plaque lipid and macrophage content in apolipoprotein E-deficient mice—Potential implications for acute plaque stabilization. *Circulation.* **103**: 3047–3050.
32. Ameli, S., A. Hultgardh-Nilsson, B. Cercek, P. K. Shah, J. S. Forrester, H. Ageland, and J. Nilsson. 1994. Recombinant apolipoprotein A-I Milano reduces intimal thickening after balloon injury in hypercholesterolemic rabbits. *Circulation.* **90**: 1935–1941.
33. Nissen, S. E., T. Tsunoda, E. M. Tuzcu, P. Schoenhagen, C. J. Cooper, M. Yasin, G. M. Eaton, M. A. Lauer, W. S. Sheldon, C. L. Grines, et al. 2003. Effect of recombinant apoA-I milano on coronary atherosclerosis in patients with acute coronary syndromes: a randomized controlled trial. *JAMA.* **290**: 2292–2300.
34. Alaupovic, P. 1996. Significance of apolipoproteins for structure, function, and classification of plasma lipoproteins. *Methods Enzymol.* **263**: 32–60.
35. Ogawa, Y., and C. J. Fielding. 1985. Assay of cholesteryl ester transfer activity and purification of a cholesteryl ester transfer protein. *Methods Enzymol.* **111**: 274–285.
36. Fielding, C. J., R. J. Havel, K. M. Todd, K. E. Yeo, M. C. Schloetter, V. Weinberg, and P. H. Frost. 1995. Effects of dietary cholesterol and fat saturation on plasma lipoproteins in an ethnically diverse population of healthy young men. *J. Clin. Invest.* **95**: 611–618.
37. de la Llera Moya, M., V. Atger, J. L. Paul, N. Fournier, N. Moatti, P. Giral, K. E. Friday, and G. Rothblat. 1994. A cell culture system for screening human serum for ability to Promote cellular cholesterol efflux. Relations between serum components and efflux, esterification, and transfer. *Arterioscler. Thromb.* **14**: 1056–1065.
38. Koritnik, D. L., and L. L. Rudel. 1983. Measurement of apolipoprotein A-I concentration in nonhuman primate serum by enzyme-linked immunosorbent assay (ELISA). *J. Lipid Res.* **24**: 1639–1645.
39. Colvin, P. L., E. Moriguchi, P. H. Barrett, J. S. Parks, and L. L. Rudel. 1999. Small HDL particles containing two apoA-I molecules are precursors *in vivo* to medium and large HDL particles containing three and four apoA-I molecules in nonhuman primates. *J. Lipid Res.* **40**: 1782–1792.
40. Mintz, G. S., S. E. Nissen, W. D. Anderson, S. R. Bailey, R. Erbel, P. J. Fitzgerald, F. J. Pinto, K. Rosenfield, R. J. Siegel, E. M. Tuzcu, et al. 2001. American College of Cardiology Clinical Expert Consensus Document on Standards for Acquisition, Measurement and Reporting of Intravascular Ultrasound Studies (IVUS). A report of the American College of Cardiology Task Force on Clinical Expert Consensus Documents. *J. Am. Coll. Cardiol.* **37**: 1478–1492.
41. Jolley, C. D., L. A. Woollett, S. D. Turley, and J. M. Dietschy. 1998. Centripetal cholesterol flux to the liver is dictated by events in the peripheral organs and not by the plasma high density lipoprotein or apolipoprotein A-I concentration. *J. Lipid Res.* **39**: 2143–2149.
42. Neufeld, E. B., J. A. Stonik, S. J. Demosky, C. L. Knapper, C. A. Combs, A. Cooney, M. Comly, N. Dwyer, J. Blanchette-Mackie, A. T. Remaley, et al. 2004. The ABCA1 transporter modulates late endocytic trafficking: insights from the correction of the genetic defect in Tangier disease. *J. Biol. Chem.* **279**: 15571–15578.
43. Gylling, H., G. L. Vega, and S. M. Grundy. 1992. Physiologic mechanisms for reduced apolipoprotein A-I concentration associated with low levels of high density lipoprotein-cholesterol levels in patients with normal plasma lipids. *J. Lipid Res.* **33**: 1527–1539.
44. Nanjee, M. N., J. R. Crouse, J. M. King, R. Hovorka, S. E. Rees, E. R. Carson, J. J. Morgenthaler, P. Lerch, and N. E. Miller. 1996. Effects of intravenous infusion of lipid-free apo A-I in humans. *Arterioscler. Thromb. Vasc. Biol.* **16**: 1203–1214.
45. Chetiveaux, M., F. Lalanne, G. Lambert, Y. Zair, K. Ouguerram, and M. Krempf. 2006. Kinetics of preβ1 HDL and αHDL in type II diabetic patients. *Eur. J. Clin. Invest.* **36**: 29–34.
46. Paterno, R. R., A. Postiglione, A. Hubsch, I. Andresen, and M. G. Lang. 2004. Reconstituted high-density lipoprotein exhibits neuroprotection in two rat models of stroke. *Cerebrovasc. Dis.* **17**: 204–211.
47. Calabresi, L., G. Rossoni, M. Gomaraschi, F. Sisto, F. Berti, and G. Franceschini. 2003. High-density lipoproteins protect isolated rat hearts from ischemia–reperfusion injury by reducing cardiac tumor necrosis factor-alpha content and enhancing prostaglandin release. *Circ. Res.* **92**: 330–337.
48. Marchesi, M., E. A. Booth, T. Davis, C. L. Bisgaier, and B. R. Lucchesi. 2004. Apolipoprotein A-I_{Milano} and 1-Palmitoyl-2-oleoyl phosphatidylcholine complex (ETC-216) protects the *in vivo* rabbit heart from regional ischemia-reperfusion injury. *J. Pharmacol. Exp. Ther.* **311**: 1023–1031.
49. Kaul, S., V. Rukshin, R. Santos, B. Azarbal, C. L. Bisgaier, and J. Johansson. 2003. Intramural delivery of recombinant apolipoprotein A-I_{Milano}/phospholipid complex (ETC-216) inhibits in-stent stenosis in porcine coronary arteries. *Circulation.* **107**: 2551–2554.